Electron Density of Corannulene from Synchrotron Data at 12 K, Comparison with Fullerenes

Simon Grabowsky[a], Manuela Weber[a], Yu-Sheng Chen[b], Dieter Lentz[a], Bernd M. Schmidt[a], Malte Hesse[a], and Peter Luger[a]

[a] Institut für Chemie und Biochemie/Anorganische Chemie, Freie Universität Berlin, Fabeckstraße 36a and Fabeckstraße 34 – 36, 14195 Berlin, Germany
[b] ChemMatCARS, Center for Advanced Radiation Sources, The University of Chicago, c/o Advanced Photon Source/ANL, 9700 South Cass Avenue, Bldg. 434D, Argonne, IL 60439, USA

Reprint requests to Prof. Dr. Peter Luger. Fax: +49-30-838 53464. E-mail: luger@chemie.fu-berlin.de

Z. Naturforsch. **2010**, *65b,* 452 – 460; received December 11, 2009

The electron density of corannulene, $C_{20}H_{10}$, was derived from a high-resolution synchrotron data set ($\sin\theta/\lambda$ = 1.11 Å^{-1}) measured at 12 K and from an *ab-initio* geometry optimization on the B3LYP/6-31G* level. A full topological analysis yielded atomic and bond-topological properties which were compared between experimental and theoretical findings and, as far as steric congruences exist, with corresponding fragments of the fullerene C_{70}. For the four different types of C–C bonds in corannulene, a rather close bond-order range between 1.3 and 1.8 was found indicating a considerable delocalization in this molecule. As was already found earlier in fullerene cages, the deformation density on the C–C bonds is not arranged symmetrically. There is more density located outside than inside the corannulene bowl so that in total, charge accumulation is shifted to the outer surface of the molecule. The electrostatic potential suggests an H$\cdots\pi$ stacking in the crystal which directs the relative orientation of the two crystallographically independent corannulene molecules. The positively charged rim region of one molecule is oriented almost perpendicular to the negative potential region at the bottom of a second molecule.

Key words: Electron Density, Topological Analysis, Synchrotron Radiation, Corannulene

Introduction

The fullerenes with 60 or more carbon atoms generally represent a challenge for experimental electron density (ED) work because of shortcomings in crystal size and quality, poor diffraction properties or disorder. Nevertheless, a couple of ED studies on derivatives of C_{60} fullerenes have been reported [1 – 4], and just recently a first experimental ED determination on a C_{70} fullerene, $C_{70}(C_2F_5)_{10}$ [5], was carried out. The title compound corannulene, $C_{20}H_{10}$, of which the conventional (spherical) X-ray structure has been known for a long time [6, 7], is sterically equal to the top and bottom fragments of the C_{70} molecule, which include the two five-membered rings on the local molecular fivefold axis. Corannulene also matches C_{60} fragments having a central five-membered ring. To compare data with the recently obtained results of the $C_{70}(C_2F_5)_{10}$ study [5], an ED examination of corannulene was carried out, based on a high-resolution synchrotron data set measured at 12 K on the ChemMatCARS 15 ID-B beamline of the Advanced Photon Source (APS), Argonne National Laboratory, complemented by theoretical results from B3LYP density-functional calculations with the 6-31G* basis set [8]. The experimental and theoretical ED distributions were analyzed quantitatively according to Bader's Quantum Theory of Atoms in Molecules (QTAIM) [9].

Results and Discussion

Structural properties

A schematic representation of the molecular structure of corannulene is shown in Fig. 1, giving also the chosen atom numbering scheme of the two molecules in the asymmetric unit. Due to the molecular C_{5v} symmetry, only three chemically different carbon atoms and four types of C–C bonds exist. In accordance with the notation chosen in ref. [7], we use the bond type names given in this previous paper (see also caption of Fig. 1) and the symbols H = hub, S = spoke, and R = rim for the corresponding atom types.

0932–0776 / 10 / 0400–0452 $ 06.00

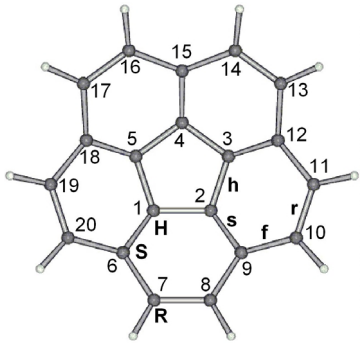

Fig. 1. Schematic representation of the corannulene structure with the atom numbering scheme used in this study. For molecules A and B in the asymmetric unit, capital letters A and B are added to the numbers. The notations used in the literature [7] for the four types of bonds are h = hub, s = spoke, f = flank, r = rim. Accordingly, the three independent atom types should be coded H = hub, S = spoke, R = rim.

From the corannulene X-ray structures reported in the literature, structural properties at five different temperatures, 293 and 203 K [6], 173 and 90 K [7] and 12 K (this work) are available. This allows a temperature-dependent consideration of properties, which has been done in the following for the isotropic equivalent displacement parameters (U_{eq}'s) and for the four C–C bond type lengths.

Average U_{eq} values for the three atom types and for the temperatures 12, 90, 173, and 293 K (the 203 K data were not used since they are not far from the 173 K results) are summarized in Table 1. As already noted in ref. [6], it can be seen on the one hand that the displacements increase slightly from H- *via* S- to R-type atoms. On the other hand, a strong decrease of U_{eq}'s is seen towards low temperatures. For example, the 12 K U_{eq}'s are by one order of magnitude smaller than the r. t. quantities and are reduced even by more than 70 % from 90 to 12 K. It follows that an X-ray diffraction experiment at this ultra-low temperature is highly preferable, however, exceptional experimental effort is needed.

With one exception, the bond lengths given in Table 2 at the temperatures 173 / 90 / 12 K agree within a one-fold standard deviation σ. The exception is the rim bond, where the 90 and 173 K values are by 0.006 and 0.009 Å, *i. e.* by 3 or 4 σ, smaller than the 12 K value. We note in this connection that in ref. [7] the difference between the maximum and minimum rim-type distance was highest (0.0095 Å) compared to all other bond lengths. Although the agreement with the 293 / 203 K entries in Table 2 is not bad, a comparison should not be made because averages of 293 and 203 K data are reported in ref. [6].

Table 1. U_{eq} values (Å^2) at different temperatures (K), averaged for H-, S-, R-type atoms and for both molecules in the asymmetric unit.

Temp. (K)	H	S	R	Ref.
293	0.057(6)	0.070(11)	0.083(10)	[6]
173	0.031(2)	0.036(3)	0.042(3)	[7]
90	0.020 (1)	0.022(1)	0.025(2)	[7]
12	0.0064(3)	0.0071(5)	0.0082(6)	this work
No. of entries	10	10	20	

Table 2. Comparison of bond lengths (Å) obtained at different temperatures, averaged for the four bond types and for both molecules.

Temp. (K)	hub	spoke	flank	rim	Ref.
av 293 / 203[a]	1.413(3)	1.391(4)	1.440(2)	1.402(5)	[6]
173	1.414(2)	1.378(2)	1.444(2)	1.380(2)	[7]
90	1.415(2)	1.379(1)	1.446(2)	1.383(2)	[7]
12	1.415(1)	1.379(1)	1.445(1)	1.389(1)	this work
No. of entries	10	10	20	10	
B3LYP/6-31G*	1.4165	1.3846	1.4483	1.3896	

[a] Corrected for libration effects.

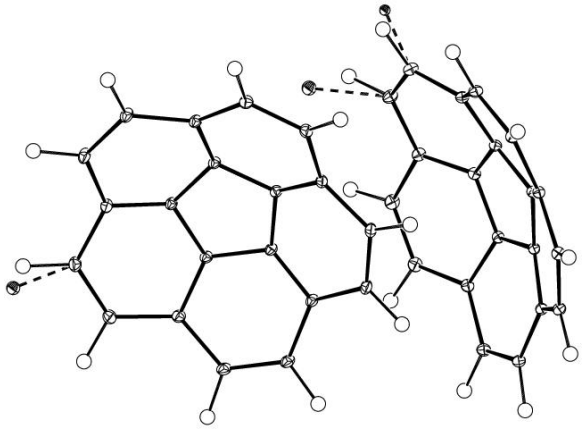

Fig. 2. Structures of the two independent molecules of corannulene at 12 K (ORTEP-III representation [10]). Anisotropic displacement parameters of carbon atoms are displayed at a 50 % probability level, hydrogen atoms as spheres of arbitrary radius.

It has already been mentioned in ref. [7] that the optimized geometry of a B3LYP/6-31G* calculation reproduces the X-ray structure results practically within the experimental error; see last line of Table 2.

The molecular structures of both crystallographically independent molecules are displayed in Fig. 2. As will be outlined below (see Experimental Section), disorder was found in three C–H regions. The distances to the additional peaks in the difference syntheses were 1.38 Å in two cases and 1.78 Å in the third

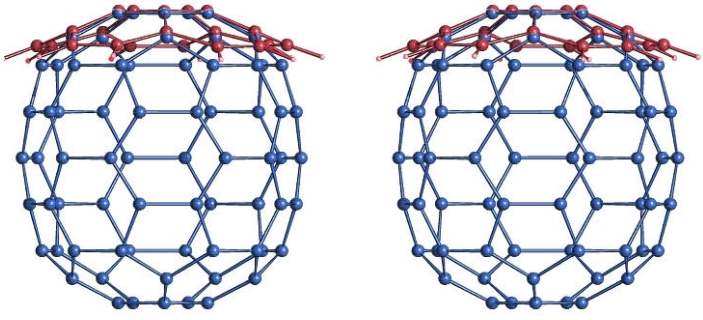

Fig. 3. Superposition of corannulene with the top five-membered ring-centered region of C_{70}; stereo representation with SCHAKAL [11].

case, being typical C–O(H) and C–Cl distances. Therefore, partially occupied additional oxygen and chlorine positions were included (see Experimental Section). We note that except for the disorder there is no significant geometric difference between the two molecules of the title compound.

It was mentioned above that the carbon skeleton of corannulene is sterically equal to the corresponding top/bottom fragments of C_{70}. We have graphically superimposed a corannulene molecule with one of these five-membered ring-centered regions of C_{70} (Fig. 3). The curvature of the corannulene bowl is more flat than in the fullerene. This can also be expressed quantitatively, using a *trans* h–s–f torsion angle (*e. g.* C3–C4–C15–C16). The average of this angle in corannulene is around 158°, but is 21° smaller in C_{70} (137°).

Bond-topological analysis

According to Bader's definition [9], bond-critical points $\boldsymbol{r}_{\mathrm{BCP}}$ (which satisfy the condition that the gradient-vector field $\nabla\rho(\boldsymbol{r})$ vanishes at $\boldsymbol{r}_{\mathrm{BCP}}$) were located for all covalent bonds. A summary of the obtained data from experiment and theory is given in Table 3.

The differences for the topological descriptors $\rho(\boldsymbol{r}_{\mathrm{BCP}})$ and $\nabla^2\rho(\boldsymbol{r}_{\mathrm{BCP}})$ between experiment and theory do not exceed 0.05 – 0.08 e Å^{-3} for $\rho(\boldsymbol{r}_{\mathrm{BCP}})$ and 2 e Å^{-5} for $\nabla^2\rho(\boldsymbol{r}_{\mathrm{BCP}})$. Taking into consideration that inconsistencies of $\sim$ 0.1 e Å^{-3} and 2 – 5 e Å^{-5} are tolerated for these quantities [12], the agreement is very acceptable.

The bond paths given in the first column in Table 3 are practically identical with the direct bond lengths given in Table 2. Only for the h and f bonds a small difference of 0.001 – 0.002 Å is seen. Hence, from these quantities no indication of a noticeable strain in the molecule exists.

Table 3. Topological properties at the bond critical points [$\rho(\boldsymbol{r}_{\mathrm{BCP}})$], averaged for h-, s-, f- and r-type bonds: First line: experiment, second line: B3LYP/6-31G* results in italics.

Type	Bond path (Å)	$\rho(\boldsymbol{r}_{\mathrm{BCP}})$ (e Å^{-3})	$\nabla^2\rho(\boldsymbol{r}_{\mathrm{BCP}})$ (e Å^{-5})	ε
h	1.4165(12)	2.131(4)	−19.25(9)	0.08
	1.4171	*2.048*	*−19.56*	*0.14*
s	1.3793(9)	2.218(3)	−19.79(7)	0.17
	1.3847	*2.173*	*−21.831*	*0.19*
f	1.4463(11)	1.943(7)	−14.8(4)	0.08
	1.4488	*1.904*	*−17.052*	*0.14*
r	1.3890(10)	2.158(4)	−19.44(8)	0.14
	1.3899	*2.108*	*−19.934*	*0.29*

However, some strain should obviously exist, because Fig. 4 illustrates that a charge displacement has taken place towards the outer surface of the corannulene bowl. Static deformation densities were generated in the plane of the five-membered ring (Fig. 4a) and in parallel planes 0.4 Å above and below this central plane, where "above" means towards the interior of the bowl (Fig. 4b) and "below" means towards the exterior (Fig. 4c). Comparison of Figs. 4b and 4c shows that higher density is found below than above the five-membered ring plane. This effect was first described in the pioneering experimental ED study of Irngartinger *et al.* [1] on a C_{60} fullerene derivative and confirmed later by theoretical ED studies on unsubstituted C_{60} [2].

For the two formal double bonds, s and r, the electron density values at the bond critical points are the highest, however, the electron density on the central five-membered ring bond h is not much lower compared for example to the r bond. The ellipticity ε, being a measure for the asphericity and hence the double bond character of a bond, is theoretically zero for a single bond and 0.25 / 0.45 for aromatic / double bonds [9]. For all bonds in corannulene, the ε values deviate considerably from zero. While from the experiment a differentiation between h and f bonds on

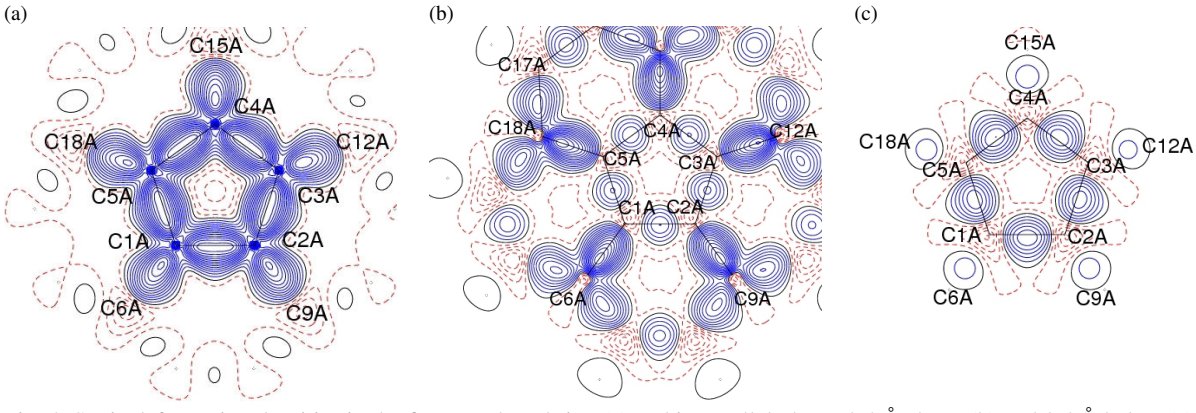

Fig. 4. Static deformation densities in the five-membered ring (a) and in parallel planes 0.4 Å above (b) and 0.4 Å below (c) the five-membered ring. Contour intervals 0.05 e Å^{-3}.

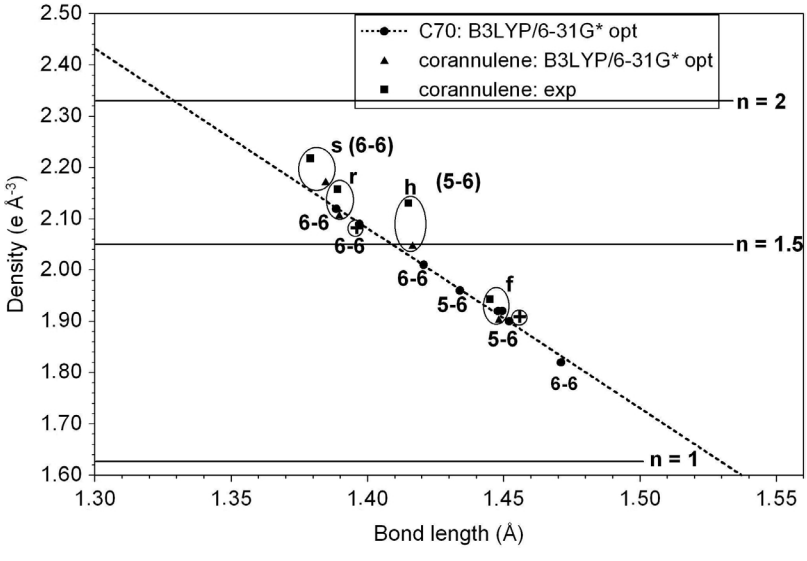

Fig. 5. Bond-topological properties $\rho(\boldsymbol{r}_{\mathrm{BCP}})$ of C_{70} obtained from B3LYP calculations and corresponding theoretical and experimental properties of coranulene. The encircled crosses refer to the two bonds in free C_{60}. Bond orders after Bader are also plotted.

one hand and s and r bonds on the other hand is seen, this differentiation is less pronounced for the theoretical values, and the $\varepsilon = 0.29$ for the theoretical r bond seems even overestimated.

For a comparison with free C_{70} the electron densities $\rho(\boldsymbol{r}_{\mathrm{BCP}})$ of the eight chemically different C–C bonds of this fullerene and the corresponding quantities of coranulene are plotted *versus* the corresponding bond lengths in Fig. 5. The C_{70} distributions can satisfactorily be fitted by a straight line. While the theoretical coranulene values properly fit the least-squares line of C_{70} (which holds also for the two independent C–C bonds in C_{60}), the experimental $\rho(\boldsymbol{r}_{\mathrm{BCP}})$ values of coranulene are slightly above the theoretical distribution.

If the electron density at a bond critical point is known, a topological bond order n_{B} can be calculated from an exponential relation given by Bader [9] after

$$n_{\mathrm{B}} = \exp[C_1(\rho(\boldsymbol{r}_{\mathrm{BCP}}) - C_2)]$$

where the parameters $C_1 = 1.02289$ and $C_2 = 1.64585$ were derived from an earlier theoretical calculation [13]. The s, r, and h bonds have bond orders close to or above $n_{\mathrm{B}} = 1.5$ and are in the same range as the two formal (6 – 6) double bonds in free C_{70}. The f bond with a bond order smaller than 1.5 is close to the (5 – 6) bonds cluster of C_{70} seen in Fig. 5. In total, a bond order range between 1.3 and 1.8 for the four coranulene C–C bonds clearly confirms a considerable delocalization in this molecule.

Table 4. Experimental Bader volumes and charges.

Type	V_{tot} (Å^3)	q (e)	N[a]
H	9.1(9)	−0.030(4)	10
S	9.7(4)	0.029(7)	10
R	12.4(8)	−0.092(6)	17[a]
Hydrogen	6.6(14)	0.109(3)	17[a]

[a] N = no. of entries, carbons and hydrogens at disordered sites not included.

For the five- and six-membered rings, ring critical points (RCP's) were derived from the experimental ED, yielding $\rho(\boldsymbol{r}_{RCP})$ / $\nabla^2\rho(\boldsymbol{r}_{RCP})$ = 0.38 e Å^{-3} / 6.6 e Å^{-5} for the five-membered rings and 0.19 e Å^{-3} / 3.1 e Å^{-5} for the six-membered rings. As expected there is less density on the somewhat larger six-membered rings, which is in line with earlier findings for five- / six-membered rings in free C_{60} [2].

Atomic properties

After Bader's QTAIM theory [9], an atom in a molecule is defined as the union of a nuclear critical point [(3; −3) critical point] and its associated basin of attracted trajectories of the electron-density gradient-vector field $\nabla\rho(\boldsymbol{r})$ with zero-flux surfaces (ZFS) as boundaries. The integration procedure available through the XDPROP subprogram of the XD2006 program suite [14] was applied to evaluate atomic volumes and charges. The results for the atoms of the title compound are summarized in Table 4. The total experimental atomic volumes V_{tot} are defined by the interatomic boundaries in the crystal.

The volumes of the H- and S-type atoms do not differ much, they are smaller than the cage atoms of the free fullerenes, C_{60} and C_{70}, where volumes of 11.0 Å^3 for C_{60} [3] and a range of 10.6 – 10.8 Å^3 for C_{70} [5] were obtained from theory. As could be expected, the R-type atoms, where the nearest neighbors are two carbon atoms (instead of three) and one hydrogen atom are considerably larger with V_{tot} = 12.4(8) Å^3. Although the atomic charge separation in corannulene is not very strong, it is stronger than in free C_{60} and C_{70}, where the atomic charges are practically zero. In corannulene the inner atoms of type H and S compensate exactly their small opposite charges of ±0.03 e. The outer atoms of type R are more negatively charged (−0.09 e) to compensate the positive charges of the hydrogen atoms. It follows that the existence of corannulene as a hydrocarbon causes a small but noticeable polarization which the free fullerenes as pure carbon compounds are lacking.

Table 5. Summary of selected bond topological and atomic properties from the experimental ED of $C_{70}(C_2F_5)_{10}$.

Type[a]	Bond path (Å)	$\rho(\boldsymbol{r}_{BCP})$ (e Å^{-3})	N[b]
h_1	1.43(4)	2.0(2)	6
h_2	1.55(1)	1.55(3)	4
s_1	1.383(8)	2.11(6)	6
s_2	1.52(1)	1.66(4)	4
f_1	1.43(3)	1.56(15)	13
f_2	1.536(7)	1.57(7)	7
r_1	1.38(1)	2.16(9)	7
r_2	1.504(4)	1.67(5)	3
	V_{tot} (Å^3)	q (e)	
H	9.6(6)	0.097(7)	8
S	10.2(15)	0.09(11)	8
R	10.1(12)	0.04(7)	17

[a] h1, . . . , r1 bonds: no C_2F_5 addend involved, h2, . . . , r2 bonds: one of the carbons carries a C_2F_5 group; [b] N = no. of entries.

Comparison with $C_{70}(C_2F_5)_{10}$

A comparison with the recently determined experimental ED of $C_{70}(C_2F_5)_{10}$ has to be considered with care. Although h-, s-, f-, and r-type bonds can also be identified in the top/bottom fragments of the C_{70} body, seven of the 40 atoms in question carry a C_2F_5 addend, and the atoms forming the r bonds in the fullerene are bonded to a third carbon instead of hydrogen in corannulene. Nevertheless, the averaged results for $C_{70}(C_2F_5)_{10}$ (Table 5) show that for bonds not affected by an addend to one of the contributing carbons (h_1-, s_1-, f_1-, r_1-type bonds) the agreement with the experimental corannulene results is quite good with a tendency to higher $\rho(\boldsymbol{r}_{BCP})$ values for corannulene. The bonds where one of the contributing atoms is additionally bonded to a C_2F_5 groups (h_2-, s_2-, f_2-, r_2-type bonds) are all significantly longer with lower BCP densities, so that in total, charge is shifted to the electronegative exo-cage groups. With respect to atomic properties, practically no differentiation between H-, S-, and R-type atoms can be made for the C_{70} compound. As mentioned in ref. [5], the cage atoms which do not carry a C_2F_5 addend have almost uniform volumes around 10 Å^3 and charges close to zero, so that their atomic properties are very similar to the ones of the H and S atoms in corannulene.

Electrostatic potential

Fig. 6 depicts a representation of the electrostatic potential (EP) [15] of molecules A and B of the title compound mapped on the *iso*-surface of the ED at a value of 0.0067 e Å^{-3} (0.001 au). The visualization was generated with MOLISO [16]. The color scale in

Table 6. Politzer analysis [17] of the EP on the ED *iso*-surface at 0.0067 Å^{-3} (0.001 au) for $C_{60}F_{18}$ [3], for $C_{70}(C_2F_5)_{10}$ [5], and for the title compound.

	$C_{60}F_{18}$	$C_{70}(C_2F_5)_{10}$	corannulene
V_s^+ (e Å^{-1})	0.214	0.190	0.046
V_s^- (e Å^{-1})	−0.115	−0.065	−0.034
Π (e Å^{-1})	0.164	0.140	0.041
σ_+^2 (e Å^{-1})^2	0.061	0.024	0.003
σ_-^2 (e Å^{-1})^2	0.044	0.020	0.002

Fig. 6 indicates that there are only small EP differences in the molecules which is in line with the small atomic charge differences discussed in the previous section. The bottom of the corannulene bowl exhibits a slightly negative region with a gradient towards the rim region where the positively charged hydrogens cause the positive EP. Fig. 6 illustrates an H$\cdots\pi$ stacking: The EP distribution obviously directs the relative orientation of molecules A and B. Molecule A is oriented almost perpendicular to the outside bottom of molecule B with a shortest intermolecular distance of H11A to the five-membered ring atom C1B of 2.69 Å, so that positively charged hydrogens of molecule A face the negative EP of the outside bottom of molecule B. A similar situation exists also for the EP of molecule A, where the inside bottom is approached by hydrogens of molecule B. The shortest H$\cdots$C distance in this case is 2.75 Å.

Table 6 shows the results of a quantitative analysis of the EP on the given ED *iso*-surface according to Politzer *et al.* [17] for the title compound and, for comparison, for the previously examined C_{60} fullerene $C_{60}F_{18}$ [3] and also for $C_{70}(C_2F_5)_{10}$ [5]. The positive and negative average potential values V_s^+ and V_s^-, the average deviation Π from the overall average potential and the corresponding variances were calculated as given in ref. [18]. V_s^+ and $|V_s^-|$ are largest for $C_{60}F_{18}$ followed by the C_{70} fullerene, indicating a rather strong polarization for these two compounds caused by the electronegative fluorine and C_2F_5 addends. This is also supported by the larger Π values, compared to the title compound.

Conclusion

Based on bright synchrotron primary radiation, a high resolution data set to sin θ/λ = 1.11 Å^{-1} could be collected on a crystal having a volume of only $1.5\cdot10^{-3}$ mm^3. The displacement parameters at the extremely low temperature of 12 K are favorably small, in fact by more than 70 % smaller than of data collected at 90 K. This strongly reduced thermal motion is a prerequisite for ED experiments to measure a large amount of high-order reflections above the background. Hence, it can be concluded that optimum experimental conditions provided data for a reliable determination of the ED of the title compound and for a detailed topological analysis even with a crystal of very low dimensions. With respect to the results, it can be concluded that

- for the molecular geometry, agreement with previous X-ray analyses was found. The tendency that smaller displacements observed at ultra-low temperatures lead to longer bonds, as was sometimes reported in the literature [19], could not be confirmed from the 12 K data of corannulene. Only for the outer rim type bonds, the bonds are marginally longer than in the 90 K study;
- as far as steric coincidence with the C_{70} fullerene exists, the bond topological properties are comparable;
- the strain in the corannulene bowl is visible by an asymmetric distribution of the deformation density on the molecular surface which is shifted to the outside, so that the surface of the title molecule is similar to that found earlier for the C_{60} cage. This is consistent with the observation of preferred *exo*-metal binding in corannulene complexes [20];
- as originally proposed by Barth and Lawton [21], the slightly negative region at the bottom of the bowl may be caused by small contributions of mesomeric resonance forms, tending to an inner cyclopentadienyl anion and an outer cyclopentadecaheptenyl cation (this annulene within an annulene structure was reflected in the name of corannulene as well).

Experimental Section

X-Ray experiments and multipole refinements

Corannulene was prepared by a slightly modified procedure of the original three-step synthesis of Scott *et al.* [22] and the improved synthesis published by Stoddart *et al.* [23]. The final step was performed using an apparatus described elsewhere [24] for the flash vacuum pyrolysis (FVP). Single crystals were grown by slow evaporation of a cyclohexane solution, suitable single crystals were pre-selected under a polarizing microscope.

A high-resolution X-ray data set was measured with synchrotron radiation (ChemMatCARS 15 ID-B beamline of the Advanced Photon Source (APS), Argonne, USA) at 12 K with a Pinkerton-type open helium gas stream cooling device [25]. A Bruker APEXII-CCD area detector was used. The related Bruker control software [26] was employed to

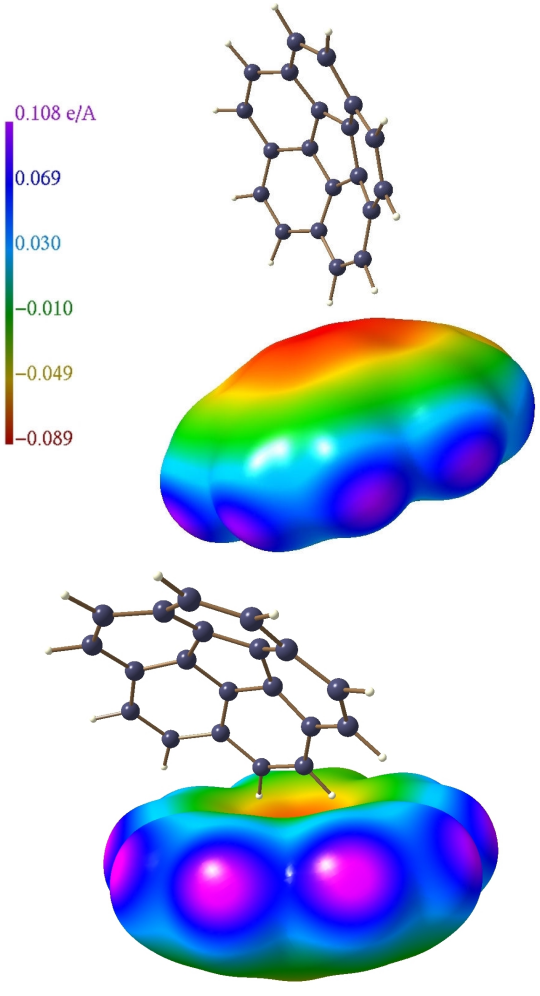

Fig. 6. Top: Electrostatic potential of molecule B of corannulene mapped on the ED *iso*-surface at 0.0067 e Å^{-3} (0.001 au). A neighboring molecule A approaching the outside bottom of molecule B is also shown; bottom: corresponding electrostatic potential of molecule A with neighboring molecule B approaching the inside bottom of molecule A. Drawings generated with MOLISO [16].

operate the data collection. At a crystal to detector distance of 50 mm, a total of eight runs were carried out following the protocol summarized in Table 7. In all runs, ω-scans were performed with frame-to-frame increments $\Delta\omega = 0.3°$. The exposure time for the whole data collection was 6.5 h. The Bruker APEXII data-processing software [26] was used for the integration of the detector data, for data reduction the SADABS and XPREP routines were applied. For a summary of crystallographic and experimental data, see Table 8.

Although the crystal structure of corannulene was known, it was decided to redetermine and rerefine the structure from the 12 K data set. During the spherical refinement, three additional maxima close to the hydrogen positions at C19A, C19B and C20B were found with distances close to 1.38 Å to C19A and C19B and 1.78 Å to C20B. Since these are quite precisely C–O(H) and C–Cl bond lengths, the maxima were interpreted as partially occupied oxygen and chlorine atoms, which seemed reasonable from the preparative work mentioned above, using 7,10-bis(1-chlorovinyl)fluoranthene as corannulene precursor for the FVP.

Table 7. Data collection strategy for corannulene.

Run no.	2θ (deg)	ω (start) (deg)	time/frame (sec.)	No. of frames
1	−25	−180	0.3	1200
2	−40	−180	2.0	1200
3	−40	−140	2.0	1200
4	−25	−160	0.3	600
5	−25	−140	0.3	600
6	−10	−170	0.3	600
7	−10	−150	0.3	600
8	−40	−220	0.5	600

Table 8. Crystal structure data for the title compound corannulene.

Formula	$C_{20}H_{10}$
M, g mol^{-1}	283.00
Crystal system	monoclinic
Space group	$P2_1/c$
Z	8
T, K	12
a, Å	13.100(5)
b, Å	11.569(5)
c, Å	16.177(5)
β, deg	102.034(5)
V, Å^3	2397.8
ρ, g cm^{-3}	1.57
μ, mm^{-1}	0.1
Crystal shape	cuboid
Crystal dimensions, mm^3	$0.14 \times 0.13 \times 0.08$
Synchrotron radiation λ, Å	0.41328
$(\sin\theta/\lambda)_{max}$, Å^{-1}	1.11
Collected reflections	205513
Completeness, %	90.8
Unique reflections	25745
Redundancy	7.25
R_{int}	0.0737
Observed reflections [$F_o \geq 4\sigma(F_o)$]	20187
$R_1[F_o \geq 4\sigma(F_o)]$	0.0435
R_1 (all data)	0.0525
wR_2	0.1223
Gof	1.072
Multipole refinement:	
$R(F)$	0.0287
$R_{all}(F)$	0.0410
$R_w(F)$	0.0286
$R(F^2)$	0.0407
$R_{all}(F^2)$	0.0440
$R_w(F^2)$	0.0569
Gof	1.81
N_{ref}/N_v	45.3

In the further course of spherical refinement, the occupancies of these extra atoms refined to rather small amounts, 0.070 and 0.032 for O and 0.013 for Cl. Occupancies of the hydrogen atoms at these sites were also refined resulting in values slightly smaller than one.

This spherical model was taken to establish the starting parameters for the subsequent aspherical atom analysis, which was based on the Hansen-Coppens multipole formalism [27] implemented in the XD2006 program package [14]. The atomic electron density $\rho_a(\boldsymbol{r})$ in this model is calculated according to

$$\rho_a(r) = \rho_{core}(r) + P_v \kappa^3 \rho_{val}(\kappa r) + \sum_{l=0}^{l\max} \kappa'^3 R_1(\kappa' r) \sum_{m=-1}^{1} P_{lm} Y_{lm}(\theta, \phi) \quad (1)$$

where the first two terms represent the spherical core and valence density and the last term accounts for aspherical contributions. In all refinements, the quantity $\sum_H w_H(|F_o(H)| - k|F_c(H)|)^2$ was minimized by using the statistical weights, $w_H = \sigma(F_o(H))^{-2}$, and only those structure factors which met the criterion $F_o(H) > 4\sigma(F_o(H))$ were included.

The multipole model was expanded up to the hexadecapole level (l = 4) for all atoms except for the disordered H, O, and Cl atoms bonded to C19A, C19B, and C20B, for which only the monopole level was used. Moreover, for these atoms positional, isotropic displacement parameters and occupancies were taken from the spherical refinement and kept fixed. Two expansion / contraction parameters (κ) were introduced and refined for the carbon atoms, one for the H and S atoms and the second one for the R atoms to account for the different nearest neighborhood (three carbons for H and S, two carbons for R atoms). Mirror site symmetry was applied to all carbon atoms, with the mirror plane perpendicular to the five-membered ring for H atoms and in the plane of the six-membered rings for the S and R atoms. Within each group of H, S and R, the atoms were constrained to each other. Additionally, molecule B was constrained to molecule A. These strong symmetry and constraint applications allowed a considerable multipole parameter reduction to yield a very favorable parameter-to-reflections ratio of $N_v/N_r \approx 45$. To examine whether this model was justified, a second multipole refinement was carried out where most of the above-mentioned symmetry and constraint restrictions were released. Since neither *R* values, Gof or residual densities indicated any improvement, this less symmetric model was not further considered, and all properties described in the discussion section were derived from the model with the symmetry / constraint applications as described above. For this model, the refinement of 20187 observed reflections $[F_o \geq 4\sigma(F_o)]$ after convergence yielded agreement factors of $R(F) = 0.029$ and $R_{all}(F) = 0.041$.

Theoretical calculations

Since no experimental ED data for free C_{60} and C_{70} exist, and to allow a comparison with the experimental results of the title compound, ED's were also derived theoretically from *ab initio* calculations at the density-functional (B3LYP) level of theory by using the GAUSSIAN 03 [8] program package. For free C_{60} and C_{70}, geometry optimizations were calculated by using the B3LYP/6-31G* basis set. For coranulene, very detailed calculations at different levels of theory were described in ref. [7]. However, to derive atomic and bond-topological properties, which were not reported in ref. [7], an *ab initio* geometry optimization was carried out for corannulene also with B3LYP/6-31G*. The topology of the electron densities was analyzed with AIMPAC [28].

CCDC 755910 contains the supplementary crystallographic data for this paper. These data can be obtained free of charge from The Cambridge Crystallographic Data Centre *via* www.ccdc.cam.ac.uk/data_request/cif.

Acknowledgements

The authors are grateful to the Deutsche Forschungsgemeinschaft (DFG) for financial support by projects Lu 222/30-2 and Le 423/13-2 within the SPP 1178 special priority program. ChemMatCARS Sector 15 is principally supported by the National Science Foundation/Department of Energy under grant number NSF/CHE-0822838. Use of the Advanced Photon Source was supported by the U. S. Department of Energy, Office of Science, Office of Basic Energy Science, under Contract No. DE-AC02-06CH11357.

[1] H. Irngartinger, A. Weber, T. Oeser, *Angew. Chem.* **1999**, *111*, 1356 – 1358; *Angew. Chem. Int. Ed.* **1999**, *38*, 1279 – 1281.

[2] A. Wagner, R. Flaig, B. Dittrich, P. Bombicz, M. Strümpel, P. Luger, T. Koritsanszky, H.-G. Krane, *J. Phys. Chem. A* **2002**, *106*, 6581 – 6590.

[3] C. B. Hübschle, S. Scheins, M. Weber, P. Luger, A. Wagner, T. Koritsanszky, S. I. Troyanov, *Chem. Eur. J.* **2007**, *13*, 1910 – 1920.

[4] L. Chęcińska, S. I. Troyanov, S. Mebs, C. B. Hübschle, P. Luger, *Chem. Commun.* **2007**, 4003 – 4005.

[5] R. Kalinowski, M. Weber, S. I. Troyanov, C. Paulmann, P. Luger, *Z. Naturforsch.* **2010**, *65b*, 1 – 7.

[6] C. E. Nordman, J. C. Hanson, *Acta Crystallogr.* **1976**, *B32*, 1147 – 1153.
[7] M. A. Petrukhina, K. W. Andreini, J. Mack, L. T. Scott, *J. Org. Chem.* **2005**, *70*, 5713 – 5716.
[8] M. J. Frisch, G. W. Trucks, H. B. Schlegel, G. E. Scuseria, M. A. Robb, J. R. Cheeseman, J. A. Montgomery, Jr., T. Vreven, K. N. Kudin, J. C. Burant, J. M. Millam, S. S. Iyengar, J. Tomasi, V. Barone, B. Mennucci, M. Cossi, G. Scalmani, N. Rega, G. A. Petersson, H. Nakatsuji, M. Hada, M. Ehara, K. Toyota, R. Fukuda, J. Hasegawa, M. Ishida, T. Nakajima, Y. Honda, O. Kitao, H. Nakai, M. Klene, X. Li, J. E. Knox, H. P. Hratchian, J. B. Cross, V. Bakken, C. Adamo, J. Jaramillo, R. Gomperts, R. E. Stratmann, O. Yazyev, A. J. Austin, R. Cammi, C. Pomelli, J. W. Ochterski, P. Y. Ayala, K. Morokuma, G. A. Voth, P. Salvador, J. J. Dannenberg, V. G. Zakrzewski, S. Dapprich, A. D. Daniels, M. C. Strain, O. Farkas, D. K. Malick, A. D. Rabuck, K. Raghavachari, J. B. Foresman, J. V. Ortiz, Q. Cui, A. G. Baboul, S. Clifford, J. Cioslowski, B. B. Stefanov, G. Liu, A. Liashenko, P. Piskorz, I. Komaromi, R. L. Martin, D. J. Fox, T. Keith, M. A. Al-Laham, C. Y. Peng, A. Nanayakkara, M. Challacombe, P. M. W. Gill, B. Johnson, W. Chen, M. W. Wong, C. Gonzalez, J. A. Pople, GAUSSIAN 03 (revision E.01), Gaussian Inc., Wallingford, CT (USA) **2004**.
[9] R. F. W. Bader, *Atoms in Molecules – A Quantum Theory*, Clarendon Press, Oxford, **1994**.
[10] M. N. Burnett, C. K. Johnson, ORTEP-III (version 1.0.2), Oak Ridge Thermal Ellipsoid Plot Program for Crystal Structure Illustrations, Rep. ORNL-6895, Oak Ridge National Laboratory, Oak Ridge, TN (USA) **1996**.
[11] E. Keller, SCHAKAL99, A Computer Program for the Graphical Representation of Molecular and Crystallographic Models, University of Freiburg, Freiburg (Germany) **1999**.
[12] B. Dittrich, M. Weber, R. Kalinowski, S. Grabowsky, C. B. Hübschle, P. Luger, *Acta Crystallogr.* **2009**, *B65*, 749 – 756.
[13] P. Luger, M. Messerschmidt, S. Scheins, A. Wagner, *Acta Crystallogr.* **2004**, *A60,* 390 – 396.
[14] A. Volkov, P. Macchi, L. J. Farrugia, C. Gatti, P. R. Mallinson, T. Richter, T. T. Koritsanszky, XD2006 – a computer program for multipole refinement, topological analysis and evaluation of intermolecular energies from experimental and theoretical structure factors, University at Buffalo, NY (USA); University of Milano (Italy); University of Glasgow (UK); CNRISTM, Milano (Italy); Middle Tennessee State University, TN (USA) **2006**.
[15] A. Volkov, H. F. King, P. Coppens, L. J. Farrugia, *Acta Crystallogr.* **2006**, *A62*, 400 – 408.
[16] C. B. Hübschle, P. Luger, *J. Appl. Crystallogr.* **2006**, *39,* 901 – 904.
[17] P. Politzer, J. S. Murray, Z. Preralta-Inga, *Int. J. Quantum Chem.* **2001**, *85*, 676 – 684.
[18] C. B. Hübschle, B. Dittrich, S. Grabowsky, M. Messerschmidt, P. Luger, *Acta Crystallogr.* **2008**, *B64,* 363 – 374.
[19] P. Luger, Ch. Andre, R. Rudert, D. Zobel, A. Knöchel, A. Krause, *Acta Crystallogr.* **1992**, *B48*, 33 – 37.
[20] M. A. Petrukhina, *Angew. Chem.* **2008**, *120*, 1572 – 1574; *Angew. Chem. Int. Ed.* **2008**, *47*, 1550 – 1552.
[21] W. E. Barth, R. G. Lawton, *J. Am. Chem. Soc.* **1966**, *88*, 380 – 381.
[22] L. T. Scott, P.-C. Cheng, M. M. Hashemi, M. S. Bratcher, D. T. Meyer, H. B. Warren, *J. Am. Chem. Soc.* **1997**, *119*, 10963 – 10968.
[23] M. W. Stoddart, J. H. Brownie, M. C. Baird, H. L. Schmider, *J. Organomet. Chem.* **2005**, *690*, 3440 – 3450.
[24] V. M. Tsefrikas, L. T. Scott, *Chem. Rev.* **2006**, *106*, 4868 – 4884.
[25] M. J. Hardie, K. Kirschbaum, A. Martin, A. A. Pinkerton, *J. Appl. Crystallogr.* **1998**, *31*, 815 – 817.
[26] APEX2, SAINT, XPREP, SADABS, Bruker Analytical X-ray Instruments Inc., Madison, WI (USA) **2004 – 2009**.
[27] N. K. Hansen, P. Coppens, *Acta Crystallogr*. **1978**, *A34*, 909 – 921.
[28] J. Cheeseman, T. A. Keith, R. W. F. Bader, AIMPAC program package, McMaster University, Hamilton, Ontario (Canada) **1992**.